



This is a repository copy of *Dynamic nuclear polarization in InGaAs/GaAs and GaAs/AlGaAs quantum dots under nonresonant ultralow-power optical excitation*.

White Rose Research Online URL for this paper:
<http://eprints.whiterose.ac.uk/102109/>

Version: Accepted Version

Article:

Puebla, J., Chekhovich, E.A., Hopkinson, M. orcid.org/0000-0002-8097-6913 et al. (4 more authors) (2013) Dynamic nuclear polarization in InGaAs/GaAs and GaAs/AlGaAs quantum dots under nonresonant ultralow-power optical excitation. *Physical Review B*, 88 (4). 045306. ISSN 2469-9950

<https://doi.org/10.1103/PhysRevB.88.045306>

Reuse

Unless indicated otherwise, fulltext items are protected by copyright with all rights reserved. The copyright exception in section 29 of the Copyright, Designs and Patents Act 1988 allows the making of a single copy solely for the purpose of non-commercial research or private study within the limits of fair dealing. The publisher or other rights-holder may allow further reproduction and re-use of this version - refer to the White Rose Research Online record for this item. Where records identify the publisher as the copyright holder, users can verify any specific terms of use on the publisher's website.

Takedown

If you consider content in White Rose Research Online to be in breach of UK law, please notify us by emailing eprints@whiterose.ac.uk including the URL of the record and the reason for the withdrawal request.



eprints@whiterose.ac.uk
<https://eprints.whiterose.ac.uk/>

Dynamic nuclear polarization in InGaAs/GaAs and GaAs/AlGaAs quantum dots under non-resonant ultra-low power optical excitation

J. Puebla¹, E. A. Chekhovich^{1,*}, M. Hopkinson², P. Senellart³, A. Lemaitre³, M. S. Skolnick¹, and A. I. Tartakovskii^{1†}

¹*Department of Physics and Astronomy, University of Sheffield, Sheffield S3 7RH, United Kingdom*

²*Department of Electronic and Electrical Engineering,*

University of Sheffield, Sheffield S1 3JD, United Kingdom and

³*Laboratoire de Photonique et Nanostructures, LPN/CNRS, Route de Nozay, 91460 Marcoussis, France*

(Dated: June 4, 2013)

We study experimentally the dependence of dynamic nuclear spin polarization on the power of non-resonant optical excitation in two types of individual neutral semiconductor quantum dots: InGaAs/GaAs and GaAs/AlGaAs. We show that the mechanism of nuclear spin pumping via second order recombination of optically forbidden ("dark") exciton states recently reported in InP/GaInP quantum dots [Phys. Rev. B 83, 125318 (2011)] is relevant for material systems considered in this work. In the InGaAs/GaAs dots this nuclear spin polarization mechanism is particularly pronounced, resulting in Overhauser shifts up to $\sim 80 \mu\text{eV}$ achieved at optical excitation power ~ 1000 times smaller than the power required to saturate ground state excitons. The Overhauser shifts observed at low-power optical pumping in the interface GaAs/AlGaAs dots are generally found to be smaller (up to $\sim 40 \mu\text{eV}$). Furthermore in GaAs/AlGaAs we observe dot-to-dot variation and even sign reversal of the Overhauser shift which is attributed to dark-bright exciton mixing originating from electron-hole exchange interaction in dots with reduced symmetry. Nuclear spin polarization degrees reported in this work under ultra-low power optical pumping are comparable to those achieved by techniques such as resonant optical pumping or above-gap pumping with high power circularly polarized light. Dynamic nuclear polarization via second-order recombination of "dark" excitons may become a useful tool in single quantum dot applications, where manipulation of the nuclear spin environment or electron spin is required.

I. INTRODUCTION

In all III-V semiconductor materials the atoms of the lattice possess non-zero nuclear spins and, as a result, have non-zero nuclear magnetic moments. Nuclear magnetism has almost no effect in classical optoelectronic semiconductor devices, but becomes an important factor in nano-scale devices, particularly in semiconductor quantum dots (QDs) where quantum degrees of freedom of single charge particles and photons are addressed. The major effect associated with nuclear magnetism is electron-nuclear (hyperfine) interaction. In quantum dots nuclear spins are capable of producing effective (Overhauser) magnetic fields as large as a few tesla, which has a dramatic effect on the quantum mechanical evolution of the electron trapped in the dot (see recent reviews¹⁻⁴). As a consequence a considerable effort has been put recently into understanding as well as controlling nuclear magnetism in semiconductor nanostructures⁵⁻⁹.

One very basic operation required to control nuclear spins is dynamic nuclear polarization (DNP) - a process that can produce a controllable non-equilibrium alignment (polarization) of nuclear spins along a certain direction (usually the direction of external magnetic field). DNP is based on the hyperfine interaction with electrons: if electrons are spin-polarized (e.g. by optical orientation) they can transfer their polarization to nuclei via flip-flops^{5,10-18}. The main obstacle in achieving high nuclear spin polarization degrees is a mismatch in Zeeman splittings of electrons and nuclei that reduces the DNP

efficiency: the electron has much larger g-factor than the nucleus and thus electron-nuclear flip-flop requires additional energy to be absorbed or emitted.

Several approaches for enhancing DNP efficiency have been demonstrated in quantum dots. For example continuous fast injection and removal of spin polarized electrons from the QD can increase the number of electron-nuclear flip-flops thus compensating for the low probability of such process. This can be achieved using non-resonant pumping with circularly polarized light of a power sufficiently high to overcome fast depolarization and optical recombination of electrons^{12,16}. Alternatively resonant optical excitation can be used to induce second-order (forbidden) processes. The key feature of this approach is direct compensation of the electron-nuclear Zeeman energy mismatch by the energy of the absorbed photon, which does not involve high population probability of the dot¹⁹⁻²².

Here we study experimentally a different mechanism of DNP, where spin polarization is transferred to nuclei from long-lived optically-forbidden ("dark") excitons in neutral QDs^{16,23,24}. Due to their long lifetime dark states can be efficiently populated even with non-resonant low-power optical pumping (~ 1000 lower than the power required to populate optically-allowed states). Furthermore, second-order recombination with simultaneous nuclear spin-flip can be a dominant process for dark exciton decay since any competing radiative recombination is very weak. As a result second-order recombination of dark excitons becomes an efficient DNP mechanism: we find that in InGaAs dots it leads to nuclear polarization characterized by Overhauser shifts

of up to $\sim 80 \mu\text{eV}$ (fully polarized nuclei would lead to the Overhauser shift in the range $120\div 300\mu\text{eV}$ depending on indium concentration^{4,25,26}). In the studied QDs such an Overhauser shift corresponds to an effective magnetic field of ~ 3 tesla. Combined with our previous work on InP/GaInP QDs¹⁶ the current results obtained on GaAs/AlGaAs and InGaAs/GaAs dots allow us to conclude that DNP via dark excitons is a phenomenon universal for neutral QDs. Due to its undemanding requirements (only low power non-resonant excitation is needed) DNP via dark excitons may become a versatile tool for controlling nuclear magnetic environment in quantum dots used to implement electron/hole spin qubits^{18,20,22,27-37}. Moreover due to its universality and high efficiency this DNP mechanism should also be taken into account in those cases where DNP needs to be avoided.

The rest of the paper is organized as follows: In Section II we describe experimental techniques and quantum dot samples used. In Sec. III we discuss photoluminescence (PL) spectra of the studied QDs with particular focus on PL of dark excitons. The main results on DNP in neutral QDs are presented in Sec. IV in the following order: In Sec. IV A we describe the techniques used to detect the Overhauser shift in single QDs using PL spectroscopy. In Sec. IV B we present experimental results on DNP in InGaAs/GaAs QDs and discuss the mechanism of DNP via second-order recombination of dark excitons. In Sec. IV C the results on DNP in GaAs/AlGaAs dots are shown and the difference of the DNP processes in InGaAs and GaAs dots is discussed. The paper is concluded in Sec. V, with additional experimental data shown in Appendix A.

II. QUANTUM DOT SAMPLES AND EXPERIMENTAL TECHNIQUES

The experiments were performed on neutral quantum dots in InGaAs/GaAs and GaAs/AlGaAs nominally undoped samples. Both structures were grown by molecular beam epitaxy (MBE). GaAs/AlGaAs interfacial dots were formed by a monolayer (ML) fluctuations of a 9 ML GaAs quantum well embedded in $\text{Al}_{0.3}\text{Ga}_{0.7}\text{As}$ barriers (further details on this sample can be found in Refs.³⁸⁻⁴⁰). The self-assembled InGaAs/GaAs dots emitting at $\lambda \sim 914$ nm were grown in a low Q-factor ($Q \sim 250$) cavity that enhances the quantum dot luminescence signal (See details in Ref.^{40,41}).

The structures were investigated using micro-photoluminescence ($\mu\text{-PL}$) spectroscopy of single neutral quantum dots. All experiments were carried out in a helium gas-exchange cryostat at $T=4.2$ K. The sample was excited by the laser focused by an aspheric lens into a spot $\sim 1 \mu\text{m}$ in diameter. The same lens was used to collect the PL signal which was then analyzed by a double spectrometer with a 1 meter working distance and equipped with a back-illuminated deep-depletion charge-

coupled device (CCD) camera. The excitation energy was chosen to match wetting layer for InGaAs dots ($E_{exc}=1.46$ eV) and was above the quantum well ground state energy ($E_{exc}=1.73$ eV) for GaAs dots. Magnetic field B_z up to 8 T was applied normal to the sample surface and parallel to the direction of PL excitation and collection (Faraday geometry).

Several individual QDs have been examined in both InGaAs (dots are labeled A1, A2, A3, etc. throughout the text) and GaAs (dots are labeled B1, B2, etc.) samples to verify the systematic nature of DNP at ultra-low optical powers. More detailed measurements have been done for five individual dots from each sample and yielded qualitatively similar results. Therefore the discussion of the main text is focused on the data obtained from dots A1, A2 and B1, while more experimental results obtained on other individual dots are presented in Appendix A.

III. PHOTOLUMINESCENCE SPECTROSCOPY OF DARK AND BRIGHT EXCITON STATES IN NEUTRAL QUANTUM DOTS

In a neutral quantum dot electrons $\uparrow(\downarrow)$ and heavy holes $\uparrow(\downarrow)$ in a spin up (down) state along the growth axis Oz form either optically forbidden "dark"^{16,23,24,40,42-51} excitons $|\uparrow\uparrow\rangle$ ($|\downarrow\downarrow\rangle$) with spin projection $+2(-2)$, or "bright" excitons $|\uparrow\downarrow\rangle$ ($|\downarrow\uparrow\rangle$) with $+1(-1)$ spin projection. The structure of the exciton eigenstates in the dot is determined by the electron-hole ($e-h$) exchange interaction^{11,42}. In quantum dots with low symmetry, exchange interaction mixes bright and dark states^{16,42,52}. As a result dark excitons gain dipole oscillator strength (due to admixture of $|\uparrow\downarrow\rangle$ and $|\downarrow\uparrow\rangle$ states) and become visible in PL.

Typical PL spectra of single neutral QDs measured in magnetic field B_z along the sample growth axis are shown in Fig. 1 for InGaAs/GaAs (a) and GaAs/AlGaAs (b) samples. For each QD two spectra are presented: at ultra-low excitation power ($P_{exc}=11$ nW for InGaAs and $P_{exc}=3.5$ nW for GaAs) and at high power ($P_{exc}=3 \mu\text{W}$ for InGaAs and $P_{exc}=0.3 \mu\text{W}$ for GaAs).

We start with discussion of the spectra measured at ultra-low powers. At these powers QD is in "linear" regime, i.e. PL intensity of all exciton lines depend linearly on excitation power P_{exc} (Refs.^{16,53}). Such regime is realized when the total probability to find the dot occupied by an exciton (in any spin state) is much less than unity ($\ll 1$). Under these conditions PL intensity of each exciton state will be determined by two factors (i) the probability for this state to be populated by the laser excitation and (ii) non-radiative escape rate (spin-flips, or non-radiative recombination). If the rate of non-radiative processes is negligibly small the relative PL intensity of each exciton state will be proportional to its initial population probability after the optical excitation. This is because each exciton (dark or bright) will have sufficient time to emit a photon if the dot is in the linear regime.

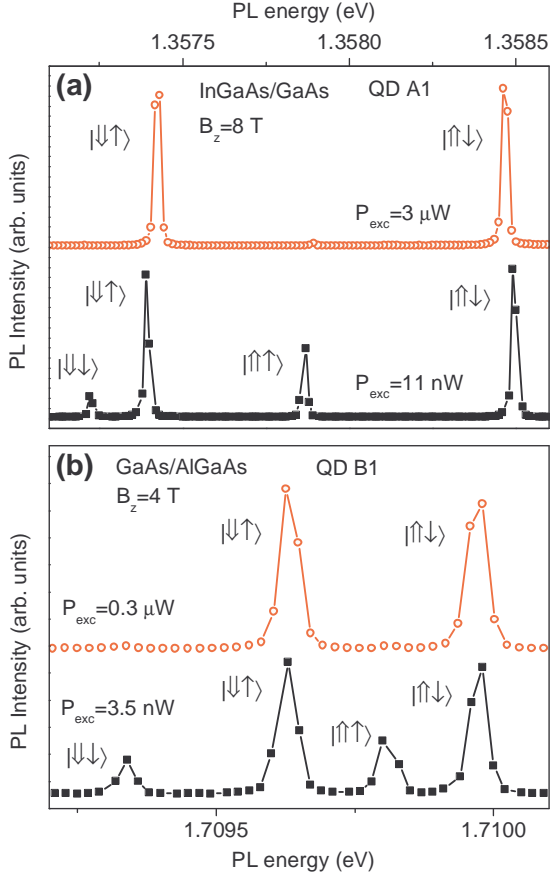


FIG. 1. Photoluminescence (PL) spectra of neutral InGaAs quantum dot A1 (a) and GaAs QD B1 (b) measured in external magnetic field applied along the sample growth axis $B_z=8$ T or $B_z=4$ T, respectively. Two spectra are shown for each quantum dot: at ultra-low optical excitation power ($P_{exc}=11$ nW for InGaAs and $P_{exc}=3.5$ nW for GaAs) and at high power ($P_{exc}=3$ μ W for InGaAs and $P_{exc}=0.3$ μ W for GaAs). Spectra are normalized to have similar maximum intensities. In a neutral quantum dot heavy hole \uparrow (\downarrow) and electron \uparrow (\downarrow) with spins parallel (antiparallel) to external field can form optically allowed "bright" states ($|\uparrow\downarrow\rangle, |\downarrow\uparrow\rangle$) and forbidden "dark" states ($|\uparrow\uparrow\rangle, |\downarrow\downarrow\rangle$) with total spin projections $J_Z = \pm 1$ and ± 2 respectively. At ultra-low excitation powers all four (bright and dark) excitons are observed in PL. At high powers PL of dark states is saturated and only bright states are observed.

As a result at ultra-low powers all four possible excitons have comparable PL intensities (Fig. 1). We note that observation of dark excitons in InGaAs/GaAs and GaAs/AlGaAs QDs at ultra-low optical powers complements the previous report for InP/GaInP quantum dots¹⁶, demonstrating that this phenomenon is not specific to a certain QD material system.

When optical excitation power is increased the PL of dark excitons saturates due to their small optical recombination rate. This saturation takes place when QD is no longer in linear regime, and dark excitons can be effectively depopulated via capture of a second exciton and

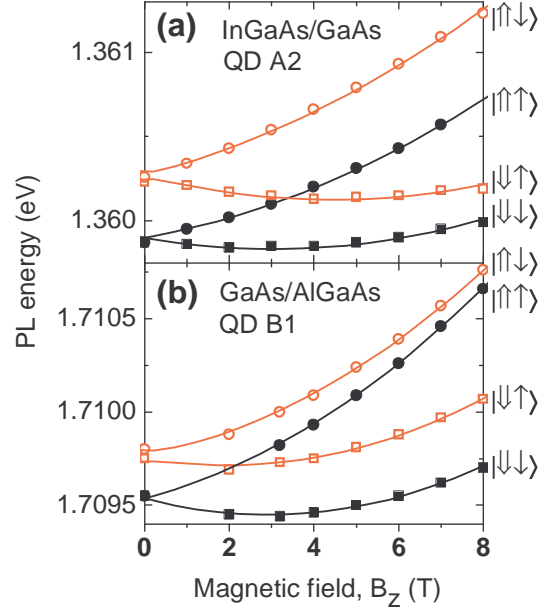


FIG. 2. Magnetic field dependence of exciton PL energies in InGaAs QD A2 (a) and GaAs QD B1 (b). Open symbols represent bright states $|\uparrow\downarrow\rangle$ (circles) and $|\downarrow\uparrow\rangle$ (squares), while solid symbols correspond to dark states $|\uparrow\uparrow\rangle$ (circles) and $|\downarrow\downarrow\rangle$ (squares). Lines show fitting using Eqs. 1 allowing electron and hole g-factors to be determined (see details in text).

formation of a biexciton state. As a result dark excitons have relatively small intensity compared to bright states at increased optical power (Fig. 1).

The dependence of PL energies of dark (E_d) and bright (E_b) exciton states on external magnetic field B_z is shown with symbols in Fig. 2 for InGaAs/GaAs (a) and GaAs/AlGaAs (b) samples. We use the following model equations for exciton energies^{16,42,51}:

$$E_b = E_0 + \kappa B_z^2 + \frac{\delta_0}{2} \pm \frac{1}{2} \sqrt{\delta_b^2 + \mu_B^2 (g_h - g_e)^2 B_z^2},$$

$$E_d = E_0 + \kappa B_z^2 - \frac{\delta_0}{2} \pm \frac{1}{2} \sqrt{\delta_d^2 + \mu_B^2 (g_h + g_e)^2 B_z^2}, \quad (1)$$

where μ_B is Bohr magneton, E_0 – QD band-gap energy, κ – diamagnetic constant, g_e (g_h) – electron (hole) g-factor, δ_0 is the splitting between dark and bright exciton doublets and δ_d (δ_b) is the dark (bright) doublet fine structure splitting. Since the Zeeman splitting of dark (bright) excitons is determined by the sum (difference) of g_e and g_h electron and hole g-factors can be determined independently from the experiment. The results of fitting using Eqs. 1 are shown in Fig. 2 with lines. We find the following fitting parameters: $\kappa \approx 7$ μ eV/T², $\delta_0 \approx 370$ μ eV, $\delta_b \approx 35$ μ eV, $g_e = -0.35$ and $g_h = 1.9$ for InGaAs/GaAs QD A2 and $\kappa \approx 10$ μ eV/T², $\delta_0 \approx 230$ μ eV, $\delta_b \approx 55$ μ eV, $g_e = 0.3$ and $g_h = 1.8$ for GaAs/AlGaAs QD B1. The splitting δ_d could not be resolved and was fixed to zero during the fitting. From the measurements on several other dots from the same samples we find very similar

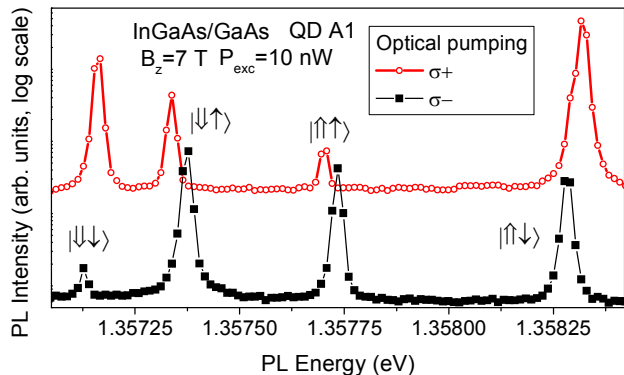


FIG. 3. Detection of nuclear spin polarization using PL in a single quantum dot. PL spectra of the InGaAs QD A1 measured at magnetic field $B_z = 7$ T and excitation power $P_{exc} = 10$ nW are shown for σ^+ (open symbols) and σ^- (solid symbols) polarized optical pumping. Logarithmic vertical scale is used to make all dark and bright exciton PL lines clearly visible in both spectra. At σ^- polarized optical pumping nuclear spin polarization is close to zero, while σ^+ pumping induces significant negative nuclear spin polarization antiparallel to external field (see Sec. IV B). This nuclear spin polarization shifts excitons with electron spin \uparrow (\downarrow) to lower (higher) energies. We use the change in energy splitting of $|\uparrow\downarrow\rangle$ and $|\downarrow\uparrow\rangle$ PL peaks as the measure of the Overhauser shift E_{OHS} .

values of κ , δ_0 , g_e and g_h while fine structure splitting δ_b changes considerably from dot to dot.

IV. DYNAMIC NUCLEAR POLARIZATION IN NEUTRAL QUANTUM DOTS AT ULTRA-LOW EXCITATION POWER

A. Detection of nuclear spin polarization in quantum dots

Nonzero average nuclear spin polarization along the external magnetic field affects QD exciton energies via the hyperfine interaction. This effect is demonstrated in Fig. 3 where PL spectra of the InGaAs QD A1 measured at $P_{exc} = 10$ nW in external magnetic field $B_z = 7$ T are shown. The two spectra were measured at σ^+ and σ^- circularly polarized optical excitation leading to different magnitudes of nuclear spin polarization on the dot (see discussion in Sec. IV B). Nuclear spin polarization shifts the energies of the exciton PL lines^{11,40}: the sign of the shift is determined by the electron spin projection (\uparrow or \downarrow) of that exciton.

In order to quantify the magnitude of the nuclear spin polarization we use the changes of the energy splitting between $|\uparrow\downarrow\rangle$ and $|\downarrow\uparrow\rangle$ excitons: $\Delta E_{|\uparrow\downarrow\rangle,|\downarrow\uparrow\rangle} = E_{|\uparrow\downarrow\rangle} - E_{|\downarrow\uparrow\rangle}$. Since the splitting $\Delta E_{|\uparrow\downarrow\rangle,|\downarrow\uparrow\rangle}$ depends on both magnetic field and nuclear spin polarization we determine the Overhauser shift as a difference

$$E_{OHS} = -(\Delta E_{|\uparrow\downarrow\rangle,|\downarrow\uparrow\rangle} - \Delta E_{|\uparrow\downarrow\rangle,|\downarrow\uparrow\rangle}^{B_N=0}), \quad (2)$$

where $\Delta E_{|\uparrow\downarrow\rangle,|\downarrow\uparrow\rangle}^{B_N=0}$ is the splitting of the bright exciton doublet corresponding to zero nuclear spin polarization. $\Delta E_{|\uparrow\downarrow\rangle,|\downarrow\uparrow\rangle}^{B_N=0}$ is measured by either keeping the sample in the dark allowing nuclear spins to relax^{52,54}, or using resonant radio-frequency excitation that depolarizes nuclear spins^{41,55}. Note the sign convention used: $E_{OHS} > 0$ corresponds to positive shift (increase in energy) of the excitons with electron in a spin-up state \uparrow . The magnitude of nuclear spin polarization can also be characterized by the effective nuclear magnetic field $B_N = E_{OHS}/(g_e\mu_B)$. By definition B_N explicitly depends on the value of electron g-factor g_e . We also note that in this work we neglect the effect of the hole-nuclear spin interaction, since its net contribution to E_{OHS} is less than 5% in the studied structures^{40,56}.

The total Overhauser shift E_{OHS} is a sum of the Overhauser shifts produced by different isotopes constituting the dot. The contributions of different isotopes can in principle be separated using nuclear magnetic resonance (NMR) techniques⁴¹. However the phenomena described in this work are not directly dependent on the way E_{OHS} is distributed between isotopes and thus we characterize nuclear spin polarization degree using total Overhauser shift E_{OHS} .

B. Dynamic nuclear polarization at ultra-low optical powers in InGaAs quantum dots

We now turn to the analysis of the mechanisms of the optically induced dynamic nuclear polarization in the studied quantum dots. For that we perform a series of power-dependent measurements on a set of different quantum dots at different magnetic fields B_z . In each measurement optical excitation power P_{exc} is stepped from high to low values in a wide range of more than six orders of magnitude. After changing P_{exc} the power is kept at this level for ~ 5 sec before PL spectrum is taken which is sufficient to achieve the steady-state nuclear polarization and eliminate any transient effects. From these spectra PL intensities of excitons as well as the Overhauser shift E_{OHS} are deduced as a function of P_{exc} . The results of such an experiment done on InGaAs QD A2 at $B_z = 7$ T are presented in Fig. 4(a) for σ^+ polarized optical pumping (open symbols) and σ^- pumping (solid symbols).

PL intensities of all four exciton transitions are shown in the top part of Fig. 4(a) (left scale). The intensities of bright excitons saturate at a power of ~ 80 μ W, while dark excitons saturate at much lower power < 5 μ W due to their significantly smaller oscillator strengths.

The power dependence of nuclear polarization in the same measurement is shown in the bottom part of Fig. 4(a) (right scale). Two distinct regimes can be observed. High-power DNP ($P_{exc} \gtrsim 5$ μ W) is characterized by monotonic power dependence and direct correspondence between the helicity of the light and the direction of the resulting nuclear field. Such pattern in the DNP power

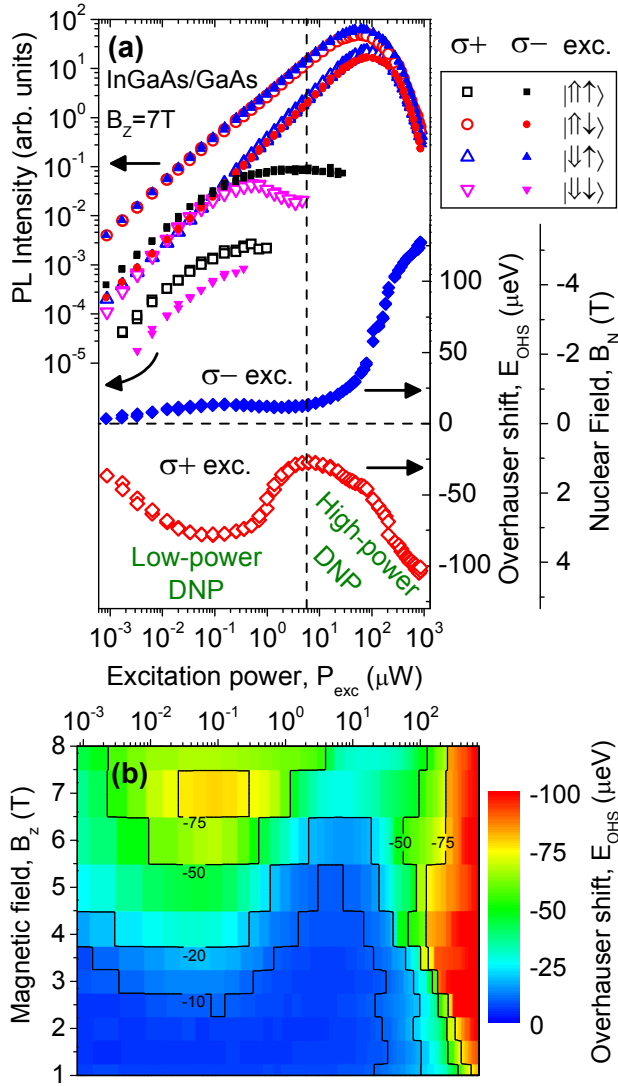


FIG. 4. (a) Results of power dependence measurements on InGaAs neutral quantum dot QD A2 at $B_z = 7$ T under σ^+ (open symbols) and σ^- (solid symbols) optical pumping. PL intensities of all bright and dark exciton states are shown at the top of the graph (left scale). Overhauser shift $E_{OHS} = -(\Delta E_{|\uparrow\downarrow\rangle,|\downarrow\uparrow\rangle} - \Delta E_{|\uparrow\uparrow\rangle,|\downarrow\downarrow\rangle}^{B_N=0})$ is shown at the bottom of the graph with diamonds (right scale). Additional scale on the right shows effective nuclear field B_N . Vertical dashed line at $P_{exc} \sim 5 \mu\text{W}$ shows an approximate boundary between two distinct nuclear spin pumping mechanisms: low-power DNP via second order recombination of dark excitons and high-power DNP due to spin transfer from spin polarized excitons/electrons (see explanation in the text). (b) Contour-plot of the power dependence of E_{OHS} on P_{exc} and B_z measured for QD A2 under σ^+ optical pumping. Low-power DNP is observed in a range of large magnetic fields with the maximum $|E_{OHS}|$ achieved at $B_z = 7$ T and $P_{exc} \approx 100$ nW.

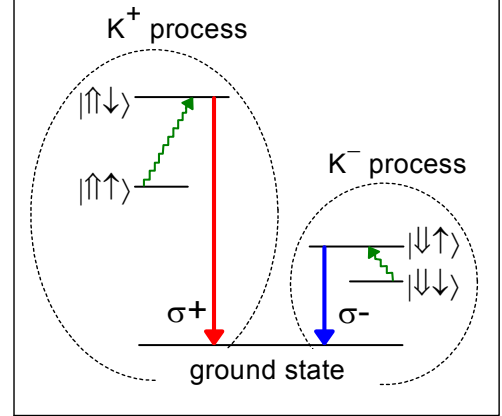


FIG. 5. Energy level diagram of a neutral exciton in an InGaAs/GaAs QD at high magnetic field $B_z \sim 7$ T. Vertical arrows show circularly polarized optical transitions due to recombination of the bright $|\uparrow\downarrow\rangle$ and $|\downarrow\uparrow\rangle$ excitons. Zigzag arrows show transitions between dark ($|\uparrow\uparrow\rangle$ and $|\downarrow\downarrow\rangle$) and bright excitons induced by electron-nuclear hyperfine interaction. Two second-order processes K^+ and K^- are highlighted: each process starts from a QD populated by a dark exciton ($|\uparrow\uparrow\rangle$ or $|\downarrow\downarrow\rangle$) respectively) and changes total nuclear spin polarization on the dot by $+1$ or -1 respectively (see detailed explanation in Sec. IV B).

dependence is well studied^{3,16,38,57}. In this regime σ^+ (σ^-) optical pumping results in negative (positive) Overhauser shift E_{OHS} which exceeds $-100 \mu\text{eV}$ ($+120 \mu\text{eV}$), corresponding to effective nuclear field in excess of $+4$ T (-5 T). However these large values of E_{OHS} are achieved only at very large pumping powers $P_{exc} \sim 1000 \mu\text{W}$ for which exciton luminescence is saturated and suppressed (Fig. 4). Thus high-power DNP can not be ascribed to ground state excitons and is likely to be a result of nuclear spin polarization transfer from delocalized spin polarized electrons in the wetting layer or highly excited QD states¹⁶.

A significantly different nontrivial pattern is observed in the low-power DNP regime ($P_{exc} \lesssim 5 \mu\text{W}$). At σ^+ pumping Overhauser shift depends non-monotonically on the excitation power with minimum $E_{OHS} \approx -80 \mu\text{eV}$ observed at a very low power of $P_{exc} \approx 100$ nW. We note that with the high-power DNP the same magnitude of E_{OHS} can only be achieved for excitation powers at least 3000 times higher.

Significant nuclear spin polarization observed at low excitation powers can be explained by nuclear spin pumping via second-order recombination of the dark excitons. This mechanism is similar to that observed in InP/GaInP dots as reported in our previous work (Ref.¹⁶). Figure 5 gives a schematic explanation. DNP takes place via transfer of spin polarization from electrons to nuclei which requires electron to flip its spin. In neutral excitons this requires conversion from a bright to a dark state or vice versa. The electron spin-flips going in opposite directions lead to increase or decrease of the total nuclear

spin polarization. However dark states have significantly longer lifetimes making the processes starting from dark states dominant.

There are two such processes^{16,23}. The first one denoted K^+ in Fig. 5 is possible if QD is occupied with $|\uparrow\uparrow\rangle$ dark exciton: electron can make a virtual flip converting exciton into a $|\uparrow\downarrow\rangle$ bright state and simultaneously increasing total nuclear spin polarization by +1 (zigzag line in the left half of Fig. 5). At the second stage the virtual $|\uparrow\downarrow\rangle$ exciton recombines emitting σ^+ polarized photon. The other process (K^-) starts from the $|\downarrow\downarrow\rangle$ dark exciton and goes via virtual $|\downarrow\uparrow\rangle$ state (zigzag line in the right half of Fig. 5). As a result of this process σ^- photon is emitted and the total nuclear spin polarization is changed by -1 . The K^+ and K^- induce nuclear spin polarization of opposite signs, thus the sign of the overall nuclear spin pumping is determined by the process with larger pumping rate.

The nuclear spin pumping rate of each of these second order processes is proportional to two quantities¹⁶: (i) population probability of the initial dark state, largely determined by laser circular polarization (optically excited holes rapidly lose their polarization during energy relaxation, while electrons maintain their spin resulting in optical orientation of dark excitons evidenced by dependence of PL intensities on excitation helicity as seen in Fig. 4(a)). (ii) the probability of the virtual electron-nuclear flip-flop, which in turn is inversely proportional to the square of the splitting between the initial and intermediate states [$\propto \Delta E_{|\uparrow\downarrow\rangle,|\uparrow\uparrow\rangle}^{-2}$ for process K^+ and $\propto \Delta E_{|\downarrow\downarrow\rangle,|\downarrow\uparrow\rangle}^{-2}$ for process K^-].

At high magnetic field [$B_z \sim 7$ T as in Fig. 4(a)] neutral exciton spectrum is asymmetric: $\Delta E_{|\downarrow\downarrow\rangle,|\downarrow\uparrow\rangle} < \Delta E_{|\uparrow\downarrow\rangle,|\uparrow\uparrow\rangle}$ (for QD A2 at $B_z = 7$ T we have $\Delta E_{|\downarrow\downarrow\rangle,|\downarrow\uparrow\rangle}^2 / \Delta E_{|\uparrow\downarrow\rangle,|\uparrow\uparrow\rangle}^2 \sim 1/5$). As a result the efficiency of the K^- process is enhanced, leading to asymmetry in low-power DNP. Furthermore at σ^+ optical pumping $|\downarrow\downarrow\rangle$ exciton is more populated than $|\uparrow\uparrow\rangle$ (this can be inferred from PL intensities shown in Fig. 4(a): in the limit of low powers PL intensity of the $|\downarrow\downarrow\rangle$ exciton is a factor of ~ 10 larger than that of $|\uparrow\uparrow\rangle$). As a result K^- process dominates over K^+ and leads to large negative $E_{OHS} \sim -80 \mu\text{eV}$ observed at low excitation power $P_{exc} \sim 100$ nW. By contrast at σ^- pumping the $|\uparrow\uparrow\rangle$ is more populated favoring the K^+ process (PL intensity of the $|\uparrow\uparrow\rangle$ exciton is a factor of ~ 70 larger compared to $|\downarrow\downarrow\rangle$). This however, is partially compensated by the large splitting $\Delta E_{|\uparrow\downarrow\rangle,|\uparrow\uparrow\rangle}$ of the initial and intermediate states involved in K^+ process. As a result of this partial compensation the overall Overhauser shift does not exceed $E_{OHS} \approx +15 \mu\text{eV}$ for σ^- excitation.

In order to examine further the mechanism of DNP in neutral InGaAs quantum dots we have performed a series of power-dependent measurements at different magnetic fields B_z . The results for QD A2 are shown in a contour plot in Fig. 4(b) where E_{OHS} is plotted as a function of P_{exc} and B_z . It can be seen that E_{OHS} induced at

low-powers ($P_{exc} \sim 100$ nW) increases significantly with magnetic field and reaches its maximum at $B_z \approx 7$ T. Such observation is in agreement with our interpretation that low-power DNP is dominated by the second order recombination of the $|\downarrow\downarrow\rangle$ exciton: as expected the $\Delta E_{|\downarrow\downarrow\rangle,|\downarrow\uparrow\rangle}$ splitting reduces with magnetic field [Fig. 2(a)] significantly enhancing the efficiency of the K^- process. By contrast the maximum $|E_{OHS}|$ achieved in the high-power DNP ($P_{exc} > 100 \mu\text{W}$) is only weakly dependent on magnetic field once it exceeds $B_z \gtrsim 2$ T.

Thus we conclude that the low-power DNP observed for InGaAs/GaAs dots (Fig. 4) has the same origin as low-power DNP previously observed in InP/GaInP QDs and the model developed in Ref.¹⁶ can be applied to InGaAs dots. There are, however, some differences in DNP induced by dark excitons in InP and InGaAs dots that are worth pointing out:

(i) In InGaAs dots K^- is the most efficient process resulting in large negative Overhauser shift E_{OHS} . By contrast in InP dots DNP via dark excitons induces positive E_{OHS} . This is due to the difference in electron and hole g-factors resulting in a different energy level structure: in contrast to InGaAs in InP dots the $\Delta E_{|\uparrow\downarrow\rangle,|\uparrow\uparrow\rangle}$ splitting is smaller than $\Delta E_{|\downarrow\downarrow\rangle,|\downarrow\uparrow\rangle}$ resulting in higher efficiency of the K^+ process in InP.

(ii) In InP dots light-polarization-independent nuclear spin pumping is observed: E_{OHS} is positive for any degree of circular polarization of light (including pure σ^+ and σ^-), whereas the sign of low-power DNP in InGaAs dots is controlled by the light helicity as described above. Such difference can be explained by much higher fidelity of optical orientation of the electron spin in InGaAs dots compared to InP: in InGaAs dots PL intensity of the dark states changes by a factor of ~ 20 when excitation is changed between σ^+ and σ^- (Fig. 4). By contrast for InP dots this factor does not exceed ~ 3 , and the balance between K^+ and K^- is controlled by the energy splitting of the initial and intermediate states rather than by the population of the initial states.

(iii) The low-power DNP process is generally more efficient in InGaAs dots. The maximum absolute value of the Overhauser shift is found to vary in the range $E_{OHS} \sim -80 \div -50 \mu\text{eV}$ in different quantum dots in the same InGaAs sample (see Appendix A) while for InP we previously observed maximum $E_{OHS} \sim 20 \div 30 \mu\text{eV}$. Such difference can be explained qualitatively if we assume significantly longer dark exciton lifetime in MBE-grown InGaAs dots compared to lower-quality MOVPE-grown InP dots, where dark state population decays due to charge fluctuations resulting from a high level of impurities. Further insight in this direction can be achieved by experiments on QD-structures where dark exciton lifetime can be manipulated directly and independently (e.g. using electric bias in Schottky-diode structures or using microwave excitation).

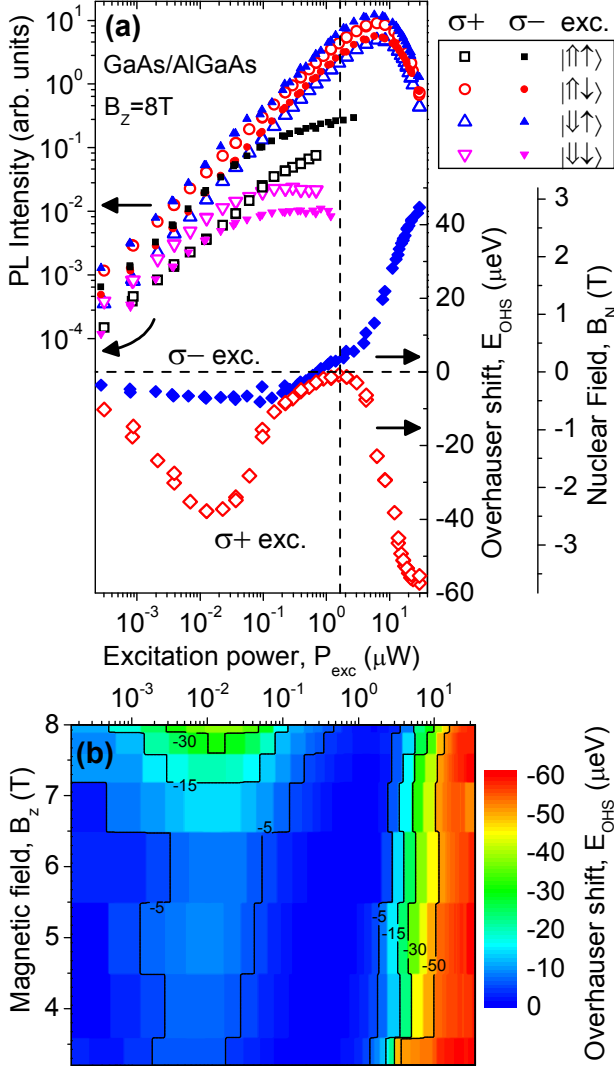


FIG. 6. (a) Results of power dependence measurements on GaAs neutral quantum dot QD B1 at $B_z = 8\text{ T}$ under σ^+ (open symbols) and σ^- (solid symbols) optical pumping. PL intensities of all bright and dark exciton states are shown at the top of the graph (left scale). Overhauser shift E_{OHS} is shown at the bottom of the graph with diamonds (right scale). Additional scale on the right shows effective nuclear field B_N . (b) Contour plot of the power dependence of E_{OHS} on P_{exc} and B_z measured for QD B1 under σ^+ optical pumping.

C. GaAs quantum dots: Modification of the low-power DNP due to electron-hole exchange interaction

We have also performed power dependence measurements on GaAs/AlGaAs QDs at different magnetic fields. The results for QD B1 are shown in Fig. 6. Similar to InGaAs dots two regimes in DNP are clearly observed. The low-power DNP mechanism reaches its peak efficiency at $B_z \approx 8\text{ T}$, $P_{exc} \approx 10\text{ nW}$ resulting in $E_{OHS} \approx 40\text{ }\mu\text{eV}$ at σ^+ polarized optical pumping.

There is a significant difference in the results for GaAs

dots compared to InGaAs: it follows from Fig. 6 that low-power DNP via dark excitons leads to negative E_{OHS} in GaAs dots despite the fact that high magnetic field reduces the $\Delta E_{|\uparrow\downarrow\rangle,|\uparrow\uparrow\rangle}$ splitting [see Fig. 2(b)] which should in principle enhance the K^+ process efficiency and lead to a net positive E_{OHS} . Furthermore, it can be seen from Fig. 6(a) that low-power DNP is more efficient at σ^+ pumping which also results in increased population of the $|\downarrow\downarrow\rangle$ dark state. This allows us to conclude that low-power DNP in QD B1 is dominated by the K^- process despite its large splitting $\Delta E_{|\downarrow\downarrow\rangle,|\downarrow\uparrow\rangle}$ of the initial and intermediate states.

These seemingly contradicting results can be explained if we take into account the role of anisotropic electron-hole exchange (Coulomb) interaction which has no significant effect in case of InGaAs dots. Quantum dot symmetry reduction can lead to mixing of bright and dark states: such mixing manifests itself as repulsion and anticrossing of the bright and dark lines in PL spectra measured in magnetic field along the growth axis^{42,58}. In the studied GaAs dots anticrossing of the $|\uparrow\uparrow\rangle$ and $|\uparrow\downarrow\rangle$ states takes place at $B_z > 8\text{ T}$ and thus could not be observed directly. However dark-bright mixing manifests itself as increased saturated PL intensity of the $|\uparrow\uparrow\rangle$ state compared to $|\downarrow\downarrow\rangle$ at $B_z = 8\text{ T}$ (see Fig. 6(a)).

As we have shown previously for InP dots the dark-bright mixing resulting from low-symmetry exchange interaction suppresses low-power DNP near the anticrossing point. Such suppression results from reduction of the dark exciton lifetime and reduction of the electron spin projections of the exciton eigenstates¹⁶. In InP and InGaAs dots dark-bright mixing results in reduction of $|E_{OHS}|$ induced by the dominant second-order process (K^- in InGaAs dots and K^+ in InP) in the small vicinity of the anticrossing point: in InGaAs QD A2 $|E_{OHS}|$ decreases when magnetic field is increased from 7 T to 8 T despite reduction of the $\Delta E_{|\downarrow\downarrow\rangle,|\downarrow\uparrow\rangle}$ splitting (see Figs. 2(a) and 4 (b)). By contrast in GaAs dot B1 the effect of the exchange interaction is much stronger and it completely suppresses the K^+ process making K^- dominant and resulting in negative E_{OHS} in the whole range of magnetic fields used (see Fig. 6(b)). Thus the increase of $|E_{OHS}|$ at $B_z = 8\text{ T}$ observed in QD B1 is due to suppression of the process with the small dark-bright splitting (K^+) which makes the process with larger dark-bright splitting (K^-) dominant.

Dark-bright mixing induced by exchange interaction depends strongly on the dot symmetry and thus can change significantly from dot to dot in the same sample⁴². As a result the magnitude of the low-power DNP also changes appreciably which has been observed in the measurements performed on several GaAs dots (see Appendix A). In particular we find that for some GaAs dots E_{OHS} induced in the low-power regime changes sign and becomes positive implying that dark-bright mixing in such dots is reduced compared to QD B1. On the other hand measurements on several InGaAs dots reveal very close values of E_{OHS} of the same sign supporting our interpre-

tation that low-symmetry exchange interaction is small in the studied InGaAs dots.

V. CONCLUSIONS

We have studied experimentally dynamic nuclear polarization under ultra-low power non-resonant optical excitation in individual InGaAs/GaAs and GaAs/AlGaAs quantum dots. We have demonstrated that nuclear spin pumping via second-order recombination of dark neutral excitons previously observed in InP/GaInP dots¹⁶ has a general nature and is found in InGaAs/GaAs and GaAs/AlGaAs dots. In InGaAs dots low-power optical pumping is found to lead to large Overhauser shifts up to $\sim 80 \mu\text{eV}$. In GaAs dots low-power DNP is systematically found to be less efficient than in InGaAs dots: we attribute this to the dark-bright exciton mixing stemming from the low-symmetry electron-hole exchange interaction. We find that the varying magnitude of the dark-bright mixing in different individual GaAs/AlGaAs dots leads to variations in the magnitude of the Overhauser shift including the change of its sign.

VI. ACKNOWLEDGMENTS

This work has been supported by the EPSRC Programme Grants EP/G001642/1 and EP/J007544/1

and the Royal Society. J. Puebla gratefully thanks CONACYT-Mexico Doctoral Scholarship.

Appendix A: Additional experimental results on dynamic nuclear polarization in neutral QDs at ultra-low power optical pumping

In order to verify systematically the nature of the low-power DNP we have performed power dependent measurements on a set of few individual quantum dots in the same InGaAs/GaAs and GaAs/AlGaAs samples. Fig. 7 shows the results for three more InGaAs dots A1, A3 and A4 (a-c) and two more GaAs dots B2 and B3 (d,e).

For InGaAs dots we find results very similar to dot A2 (Fig. 4): low power DNP results in peak $E_{OHS} \approx -70 \mu\text{eV}$ observed for σ^+ optical pumping at $B_z = 8 \text{ T}$. By contrast, we find different behavior for different GaAs dots. In QD B2 we find negative E_{OHS} for both σ^+ and σ^- optical pumping suggesting that similar to the case of QD B1 dark-bright exciton mixing strongly suppresses the K^+ process. On the other hand in QD B3 we find that the sign of the low-power DNP is controlled by the helicity of the optical excitation: under σ^- pumping which enhances $|\uparrow\uparrow\rangle$ initial population the K^+ becomes dominant leading to $E_{OHS} > 0$. The recovery of the K^+ process observed in QD B3 can be explained by the reduction of the anisotropic $e-h$ exchange interaction in this dot.

-
- * e.chekhovich@sheffield.ac.uk
 † a.tartakovskii@sheffield.ac.uk
- ¹ B. Urbaszek, *et al.*, Rev. Mod. Phys. **85**, 79 (2013).
 - ² E. A. Chekhovich, *et al.*, Nature Materials **12**, 494 (2013).
 - ³ A. S. Bracker, D. Gammon, V. L. Korenev, Semicond. Sci. Technol **23**, 114004 (2008).
 - ⁴ W. A. Coish, J. Baugh, physica status solidi (b) **246**, 2203 (2009).
 - ⁵ A. Imamoglu, E. Knill, L. Tian, P. Zoller, Phys. Rev. Lett. **91**, 017402 (2003).
 - ⁶ D. Klausner, W. A. Coish, D. Loss, Phys. Rev. B **73**, 205302 (2006).
 - ⁷ Y. Hu, F. Kuemmeth, C. M. Lieber, C. M. Marcus, Nature Nanotech. **7**, 1748 (2012).
 - ⁸ S. Nadj-Perge, S. M. Frolov, E. P. A. M. Bakkers, L. P. Kouwenhoven, Nature **468**, 1084 (2010).
 - ⁹ R. Takahashi, K. Kono, S. Tarucha, K. Ono, Phys. Rev. Lett. **107**, 026602 (2011).
 - ¹⁰ A. Abragam, *The Principles of Nuclear Magnetism* (Oxford University Press, London, 1961).
 - ¹¹ D. Gammon, *et al.*, Phys. Rev. Lett. **86**, 5176 (2001).
 - ¹² A. I. Tartakovskii, *et al.*, Phys. Rev. Lett. **98**, 026806 (2007).
 - ¹³ C. W. Lai, P. Maletinsky, A. Badolato, A. Imamoglu, Phys. Rev. Lett. **96**, 167403 (2006).
 - ¹⁴ B. Eble, *et al.*, Phys. Rev. B **74**, 081306 (2006).
 - ¹⁵ P.-F. Braun, *et al.*, Phys. Rev. B **74**, 245306 (2006).
 - ¹⁶ E. A. Chekhovich, A. B. Krysa, M. S. Skolnick, A. I. Tartakovskii, Phys. Rev. B **83**, 125318 (2011).
 - ¹⁷ V. L. Korenev, Phys. Rev. Lett. **99**, 256405 (2007).
 - ¹⁸ S. G. Carter, S. E. Economou, A. Shabaev, A. S. Bracker, Phys. Rev. B **83**, 115325 (2011).
 - ¹⁹ E. A. Chekhovich, *et al.*, Phys. Rev. Lett. **104**, 066804 (2010).
 - ²⁰ C. Latta, *et al.*, Nature Physics **5**, 758 (2009).
 - ²¹ A. Högele, *et al.*, Phys. Rev. Lett. **108**, 197403 (2012).
 - ²² X. Xu, *et al.*, Nature **459**, 1105 (2009).
 - ²³ V. L. Korenev, JETP Lett. **70**, 129 (1999).
 - ²⁴ F. Klotz, *et al.*, Phys. Rev. B **82**, 121307 (2010).
 - ²⁵ M. Gueron, Phys. Rev. **135**, A200 (1964).
 - ²⁶ B. Gotschy, G. Denninger, H. Obloh, W. Wilkening, J. Schnieder, Solid State Communications **71**, 629 (1989).
 - ²⁷ I. T. Vink, *et al.*, Nature Physics **5**, 764 (2009).
 - ²⁸ D. Stepanenko, G. Burkard, G. Giedke, A. Imamoglu, Phys. Rev. Lett. **96**, 136401 (2006).
 - ²⁹ A. V. Khaetskii, D. Loss, L. Glazman, Phys. Rev. Lett. **88**, 186802 (2002).
 - ³⁰ I. A. Merkulov, A. L. Efros, M. Rosen, Phys. Rev. B **65**, 205309 (2002).
 - ³¹ T. D. Ladd, *et al.*, Phys. Rev. Lett. **105**, 107401 (2010).
 - ³² K. D. Petersson, *et al.*, Nature **490**, 380 (2012).
 - ³³ J. Medford, *et al.*, Phys. Rev. Lett. **108**, 086802 (2012).
 - ³⁴ L. Cywiński, W. M. Witzel, S. Das Sarma, Phys. Rev. B **79**, 245314 (2009).

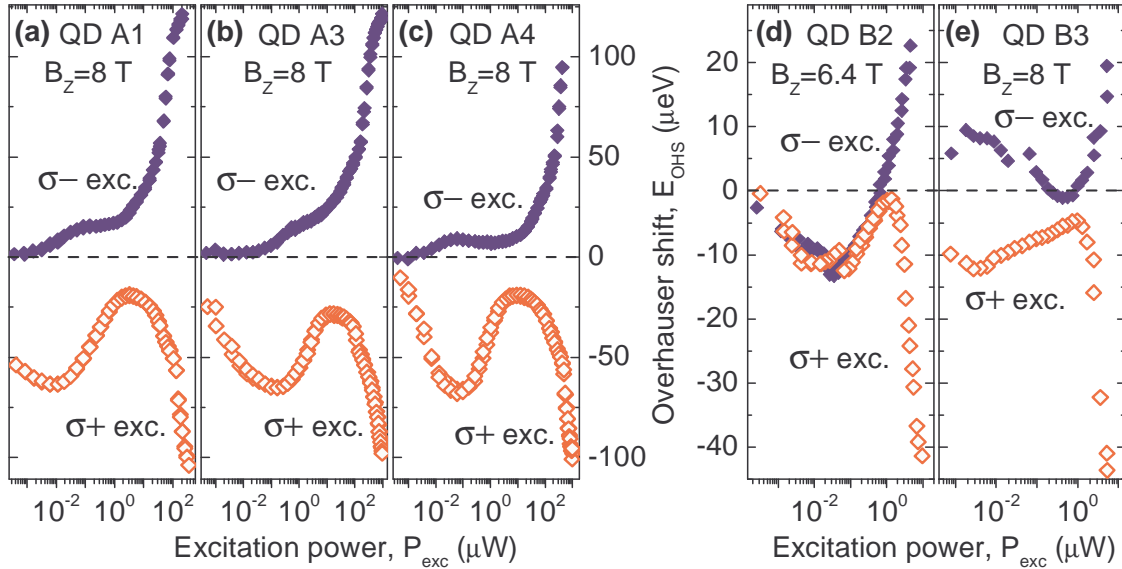


FIG. 7. Results of power dependence measurements on several individual neutral QDs from the same InGaAs and GaAs samples as reported in Figs. 4, 6. (a-c) show the data for InGaAs QDs A1, A3 and A4 measured at $B_z = 8$ T [compare to Fig. 4(a)]. (d,e) show the data for GaAs QDs B2 and B3 measured at $B_z = 6.4$ T and $B_z = 8$ T respectively [compare to Fig. 6(a)].

- ³⁵ A. Grelich, *et al.*, Phys. Rev. B **79**, 201305 (2009).
³⁶ J. M. Taylor, C. M. Marcus, M. D. Lukin, Phys. Rev. Lett. **90**, 206803 (2003).
³⁷ B. D. Gerardot, *et al.*, Natrue **451**, 441 (2007).
³⁸ A. E. Nikolaenko, *et al.*, Phys. Rev. B **79**, 081303 (2009).
³⁹ M. N. Makhonin, *et al.*, Phys. Rev. B **82**, 161309 (2010).
⁴⁰ E. A. Chekhovich, *et al.*, Nature Phys. **9**, 74 (2013).
⁴¹ E. A. Chekhovich, *et al.*, Nature Nanotech. **7**, 646 (2012).
⁴² M. Bayer, *et al.*, Phys. Rev. B **65**, 195315 (2002).
⁴³ E. Poem, *et al.*, Nature Phys. **6**, 993 (2010).
⁴⁴ E. A. Chekhovich, A. B. Krysa, M. S. Skolnick, A. I. Tartakovskii, Phys. Rev. Lett. **106**, 027402 (2011).
⁴⁵ T. Smoleński, *et al.*, Phys. Rev. B **86**, 241305 (2012).
⁴⁶ H. Kurtze, D. R. Yakovlev, D. Reuter, A. D. Wieck, M. Bayer, Phys. Rev. B **85**, 195303 (2012).
⁴⁷ S. Sancho, *et al.*, Phys. Rev. B **84**, 155458 (2011).
⁴⁸ K. F. Karlsson, *et al.*, Phys. Rev. B **81**, 161307 (2010).
⁴⁹ L. Besombes, K. Kheng, D. Martrou, Phys. Rev. Lett. **85**, 425 (2000).
⁵⁰ B. J. Wittek, *et al.*, Phys. Rev. B **84**, 195305 (2011).
⁵¹ M. Bayer, O. Stern, A. Kuther, A. Forchel, Phys. Rev. B **61**, 7273 (2000).
⁵² E. A. Chekhovich, *et al.*, Phys. Rev. B **81**, 245308 (2010).
⁵³ J. J. Finley, *et al.*, Phys. Rev. B **63**, 073307 (2001).
⁵⁴ C. Latta, A. Srivastava, A. Imamoglu, Phys. Rev. Lett. **107**, 167401 (2011).
⁵⁵ C. Bulutay, Phys. Rev. B **85**, 115313 (2012).
⁵⁶ P. Fallahi, S. T. Yilmaz, A. Imamoglu, Phys. Rev. Lett. **105**, 257402 (2010).
⁵⁷ J. Skiba-Szymanska, *et al.*, Phys. Rev. B **77**, 165338 (2008).
⁵⁸ E. A. Chekhovich, *et al.*, Phys. Rev. B **76**, 165305 (2007).